Local 5G mmWave Signal Measurement and Analysis for Spectrum Database

Hirofumi Nakajo and Takeo Fujii
Advanced Wireless and Communication Research Center (AWCC), The University of Electro-Communications
1–5–1 Chofugaoka, Chofu, Tokyo 182–8585, Japan
Email: {nakajo, fujii}@awcc.uec.ac.jp

***Abstract*—The concept of the smart spectrum has been proposed to deal with the problem of shortage of spectrum, which is a limited resource. In smart spectrum, a database is constructed based on the measured data of the radio environment to manage the spectrum, thus realizing highly efficient spectrum utilization, and its usefulness has been confirmed in several systems. On the other hand, for 5G NR signals, the database based on the smart spectrum has not been studied and its usefulness has not been confirmed. In particular, since 5G millimeter wave (mmWave) signals adopt beamforming technology, it is necessary to estimate the directivity and propagation characteristics of multiple beams. Therefore, in the database construction, we need to measure and manage not only the conventional management for each base station and frequency but also each beam. In this paper, we conduct a measurement campaign of mmWave signals from a local 5G base station in Imabari City, Ehime Prefecture, Japan, and construct a spectrum database. We also discuss the analysis results of mmWave signals based on the constructed database, including the radio propagation of each beam and the comparison with anchor band signals, and confirm the usefulness.**

***Index Terms*—Smart spectrum, spectrum database, measurement campaign, 5G, mmWave, radio map**

I. Introduction

The demand for wireless communication is increasing rapidly due to the spread of smartphones and the diversification of communication usage resulting from the development of machine-to-machine (M2M) and Internet-of-Things (IoT). According to a report by Ericsson, the total global mobile data traffic reached 49 exabytes per month at the end of 2020 and is expected to increase nearly 5 times to reach 237 exabytes per month by 2026 [1]. To deal with this exponential increase in traffic, the commercialization of the 5th generation mobile communication system (5G) has started in 2019 worldwide. 5G is the first generation of mobile communication systems that utilize high-frequency bands such as millimeter wave (mmWave) and achieves high-speed, high-capacity communication with a wide frequency bandwidth. In addition, by cooperatively operating a large number of antenna elements, it is possible to form a beam with directional characteristics (beamforming), thereby expanding the coverage area. On the other hand, a serious shortage of spectrum resources due to the increasing demand for mobile communications has become a global problem. To avoid interfering or causing interference among systems, the current policy of spectrum utilization is to allocate spectrum exclusively to certain systems. Furthermore, almost all the spectrum suitable for mobile communications is allocated to some systems. Therefore, there is a limit to the allocation of additional new systems to the limited spectrum resources. On the other hand, the spectrum allocated to existing systems is not always utilized, and there are cases where the actual temporal and spatial spectrum utilization is extremely low [2]. Such a spectrum band that is allocated to a particular system but is not utilized at a certain time or area is called white space [3], [4]. To achieve highly efficient utilization of the limited spectrum resource, it is important to establish methods for utilizing white space and framework and management techniques for spectrum utilization that prevent the generation of white space. The industry, academia, and government have been actively discussing this problem for about 20 years, and various techniques have been proposed, such as cognitive radio [5], dynamic spectrum access [6], and spectrum sharing [7]. Among the proposals, a concept called ”smart spectrum” has been proposed as one of the methods for spectrum management based on measurement data [8]. Smart spectrum aims to achieve sustainable development of wireless applications and technologies by accurately constructing a spectrum database based on measured data and managing the spectrum. The technologies that enable the smart spectrum are broadly classified into measurement, modeling, database, and management, and the smart spectrum is a framework that integrates these technologies. This prior information is utilized to determine the wireless parameters and allocate the spectrum according to the communication requirements of the wireless system and the user. The spectrum database, which forms the basis of smart spectrum, has been studied in several wireless systems (e.g., TV broadcasting, vehicle-to-everything (V2X), 4G, and wireless LAN), and its usefulness has been confirmed in terms of appropriate wireless parameter design based on statistical information of measured datasets. For example, a database of Japanese TV broadcast signals is constructed, and the transmission power of secondary users in spectrum sharing is designed to be suitable for the propagation characteristics of the actual environment, thereby improving the spectrum sharing performance [9]. Moreover, the packets of the on-board unit have been measured for V2X, which supports the prediction of reliability at a given location [10]. On the other hand, for 5G NR signals, a database based on the smart spectrum has not been studied and its usefulness has not been confirmed. In particular, for 5G mmWave signals, it is necessary to take into account the fact that multiple beams are emitted from the base station due to the adoption of beamforming technology. Therefore, to construct a database, it is required to measure and manage each beam in addition to the conventional measurement for each base station and frequency. In this paper, we conduct a measurement campaign of 5G mmWave signals for a local 5G system in Japan and construct a measurement-based spectrum database. Additionally, based on the stored datasets, we show the results of radio maps that enable visualization of the spatial radio propagation environment, analysis of the highest received signal power and its beam index in each beam at each location, comparison between mmWave signals and microwave signals, which are anchor bands, and comparison with propagation model.

This paper is organized as follows. Sect. II describes the overview of the spectrum database and the construction procedure. Sect. III explains the details of the measurement campaign. Sect. VI shows the analysis results of the measurement data. Then, we conclude this paper in Sect. V.

II. Spectrum Database

A. Geolocation Database

The spectrum database contains information on the radio environment for designing the parameters of the wireless system. One of the typical databases is the geolocation database, which is managed by the Federal Communications Commission (FCC) of the United States for spectrum sharing in TV broadcasting systems. The concept is to share the white space of the TV broadcasting spectrum band for secondary use by general wireless devices. To avoid the interference of the signals from the secondary user's wireless devices to the primary user's TV broadcasting system, the geolocation database manages the areas where the general wireless devices are allowed to transmit. The secondary user obtains the location information of its own wireless devices using GPS and queries the database for the transmission available area. The transmission available area is determined by a predetermined propagation model. However, it is difficult for the propagation model to accurately estimate the propagation environment, such as location-dependent shadowing, and errors between the propagation model and the actual environment have been reported [11], [12]. Therefore, when estimating the service area of the primary user and the transmission availability area of the secondary user by the propagation model, a large interference protection margin is set in the design of the secondary user's transmit power because both estimated areas contain errors. This is to protect the service area of the primary user, but it reduces the spectrum efficiency.

B. Measurement-based Spectrum Database

In the spectrum database construction based on the concept of the smart spectrum, it is considered to be constructed by measuring the actual radio environment to realize spectrum management with high spectrum efficiency [13]. Instantaneous received power values, GPS information (longitude, latitude), and other information measured by devices with wireless communication functions such as smartphones, wireless sensors, and vehicles are stored in a spectrum database. By utilizing the statistical information from these measurements information, it is possible to estimate the propagation environment with high accuracy and realize efficient spectrum utilization. Examples of statistical information include the average received power, the distribution of received power, and the packet delivery rate.

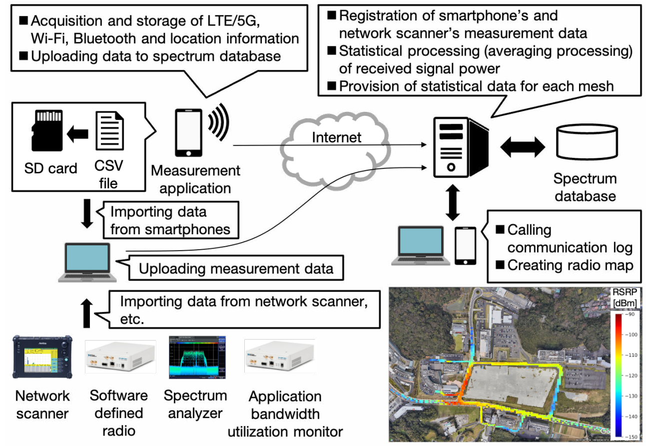

Fig. 1. Procedure for constructing spectrum database.

Fig. 1 shows an overview of the procedure for constructing spectrum database. Firstly, we measure the radio environment information of the system we need to obtain, such as LTE/5G, Wi-Fi, Bluetooth, etc., using measurement equipment or smartphones, and save the information in the internal storage. For example, the specific information to be obtained for LTE systems includes the date, time, center frequency, bandwidth, latitude, longitude, physical cell ID (PCI), and received signal power. When measuring 5G systems, we additionally obtain information on the beam index, which is the identification number of the beam. Then, the information is uploaded to the spectrum database server from a PC which is imported the acquired data or smartphones via the Internet. After that, the data uploaded to the server is registered in the database. This server processes the registered data statistically for each mesh based on the mesh code. Here, a mesh is a geographic area divided into two-dimensional squares based on latitude and longitude. Finally, the statistically processed data is output to a PC and used for various purposes. One of the purposes is to generate a radio map to confirm the propagation status of a given base station. The radio map is obtained by calculating the average value of the received signal power for each mesh and converting it into a heat map, which enables highly accurate propagation prediction at any given location. In this paper, for 5G mmWave signals, the measurement target is the synchronization signal (SS) of the SS-Block included in each beam. The SS-reference signal received power (SS-RSRP), which is the received power of the SS per resource element, is selected as the main measurement parameter. The SS-RSRP was chosen because SS is a traffic-independent signal transmitted at regular intervals and the received level of the signal from the base station is a fundamental parameter determined by the propagation environment. For microwave anchor band signals, the received signal power of the reference signal (RSRP) is measured for the same reason as for mmWave signals. When constructing the database, SS-RSRP is managed by PCI, center frequency, and beam index. The RSRP is also managed by PCI and center frequency.

III. Measurement Campaign

A. Measurement Equipment

Fig. 2 shows the configuration of the measurement equipment used in the measurement campaign. The measurement equipment consisted of one omnidirectional antenna (Anritsu's Z2039A) for 28 GHz mmWave band measurement compatible with 5G/local 5G and one omnidirectional antenna (PCTEL's OP278H) for 2.6 GHz anchor band measurement compatible with multi-band, connected to an network scanner (Anritsu's ML8780A Area tester), a GPS antenna, and a portable power supply were installed on a cart and containers. The antenna for the 28 GHz mmWave band was connected to the network scanner by a 2 m coaxial cable, and the antenna for the anchor band was directly connected to the network scanner because it was equipped with a 3.7 m cable. The network scanner can measure signals from multiple cellular systems, frequencies, and different base stations at the same time, and is a device used by combining units according to the system to be measured. In this measurement campaign, we measured local 5G mmWave signals and anchor band signals by using a mmWave measurement unit and a TD-LTE measurement unit. Since the mmWave unit can measure each beam of mmWave beamforming at once, and is suitable for highly efficient mmWave measurement and database construction, it was adopted as the network scanner in this campaign.

B. Measurement Content

A measurement campaign was conducted on Feb. to March, to construct a measurement-based spectrum database of mmWave signals of 5G NR. This campaign measured local 5G mmWave signals operated by Ehime CATV in Imabari City, Ehime Prefecture, Japan. The local 5G communication system is based on the NR system, and the frequency is 28 GHz of mmWave. The local 5G base station is located at the Itoyama observatory near the Kurushima Kaikyo Bridge in Imabari City, Ehime Prefecture, and its view is shown in Fig. 3. The anchor band base station is also located at the same observatory, a short distance away. As shown in Fig. 3, the base station is located at a high altitude observatory, and the measurement course was set to the Kurushima Kaikyo Bridge, which is the coverage area of the base station. The overall view of the measurement course is shown in Fig. 4. The measurement was conducted by pushing the cart equipped with the measurement equipment shown in Fig. 2 back and forth along the measurement course. After the measurement campaign, the CF card that had recorded the measurement data was connected to a PC, and the measurement data was registered to the spectrum database via the Internet.

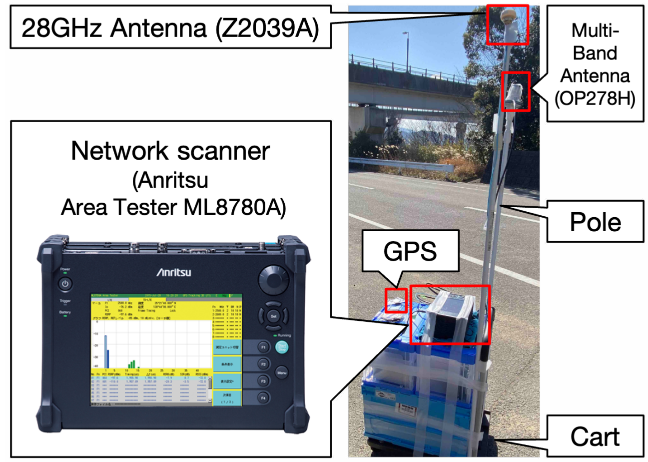

Fig. 2. Measurement equipment.

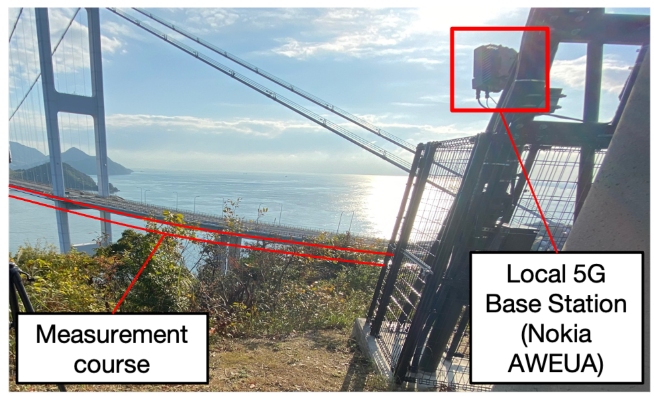

Fig. 3. Local 5G base station and measurement course.

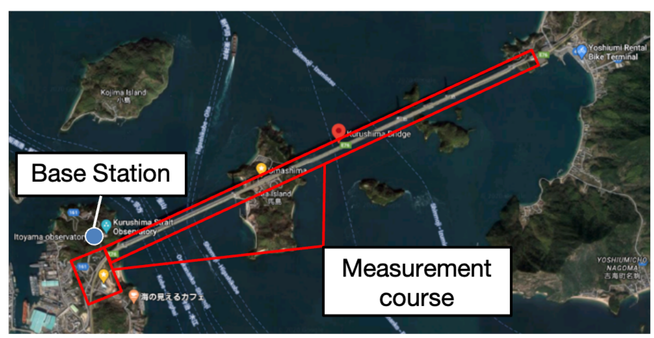

Fig. 4. Overall view of measurement course.

IV. Measurement Results

A. Examples of Radio Map

The radio maps of mmWave signals generated based on the constructed database are shown in Fig. 5 and 6. These figures show the radio maps with a PCI of 604 and beam indexes of 4 and 5, which represent the beam numbers. The antenna of the local 5G base station consists of 32 beams in total, and in this measurement campaign, we were able to measure SS-RSRP with 15 beam indexes. Therefore, we show the radio maps with beam indexes 4 and 5 as examples of radio maps of mmWave beam. This map shows the averaged SS-RSRP values of the dataset stored in the database for each mesh separated by 5 m, and the averaged SS-RSRP values are shown on a color scale from -140 dBm to -95 dBm. From Fig. 5 and 6, it can be seen that the average SS-RSRP in the mesh at each location has different values depending on the beam index. In addition, because of the high blockage loss in the high frequency band such as mmWave, there were cases where the measurement data could not be obtained when the measurement was conducted at the location where the blockage was caused by the bridge piers when viewed from the base station. This corresponds to the uncolored meshes in Fig. 5 and 6. We can also see from Fig. 5 where the high and low values of the average SS-RSRP are alternately shown near the base station. Since there is no obstacle between the point where the average SS-RSRP is low and the base station, we can assume that one of the reasons for the low value is that the beam directivity is affected in the radio map. In this Fig. 5, the beam with beam index 4 has a directivity of a side lobe, a null, and a main lobe in the order of distance to the base station, and we consider that the effect of such antenna gain is shown in the radio map. Finally, Fig. 7 shows the point where the difference in directivity between beams 4 and 5 is significantly expressed. As shown in Fig. 7, the red square is the bridge pier and the blue square is the base station, and we can see that there is a large difference in the average SS-RSRP values behind the bridge pier as seen from the base station. In the map with beam index 4, the average SS-RSRP value is around -110 dBm, while in the map with beam index 5, it is around -120 dBm. The reason for this is that the beam direction of beam index 4 is near vertical to the bridge and that of beam index 5 is near horizontal to the bridge, which may have caused the difference in the occurrence of blockage by the bridge pier. Thus, the radio maps generated for each beam clarified the directivity of the beam and the blockage.

Fig. 5. Radio map with beam index 4.

Fig. 6. Radio map with beam index 5.

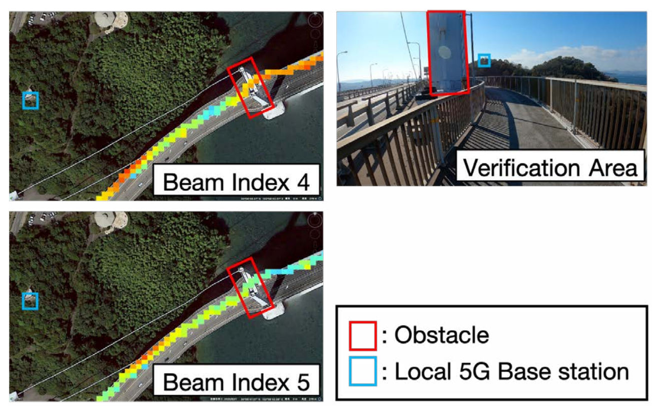

Fig. 7. Difference in directivity between beams 4 and 5.

B. Analysis of Beam Index

As confirmed in Sect. IV-A, the average SS-RSRP values are different for each beam. In this section, we analyze the highest value in the average SS-RSRP of each beam and its beam index for each meshed location. Fig. 8 shows a radio map showing the highest average SS-RSRP for each mesh among the 15 beam indexes that were measured. It can be seen from Fig. 8 that the overall average SS-RSRP decreases as the distance from the base station increase. On the other hand, the number of meshes with high average SS-RSRP increases from the radio map of beams 4 and 5 because the value of the beam with the highest average SS-RSRP among the beams emitted from the base station in various directions is mapped for each mesh. This can be considered as one of the quality confirmation indicators when the terminal communicates with the 5G base station, selecting the beam with the highest SS-RSRP for mobile communication. Then, the fluctuation graph of the highest average SS-RSRP among each beam index and its beam index is shown in Fig. 10, using the GPS logs when moving from the start position to the goal position as shown in Fig. 9. From Fig. 10, it can be seen that the highest average SS-RSRP is seen in the beam index range of 4 to 7 on the road near the start position. On the bridge near the base station, the highest values of beam indexes are 4 and 12. After passing near the base station, the values of beam index 5 and 13 are the highest as the terminal moves toward the goal position. Thus, the information on the fluctuation of the beam index of the highest SS-RSRP with the movement of the terminal is stored in the spectrum database, which can be applied to the control and management of each beam.

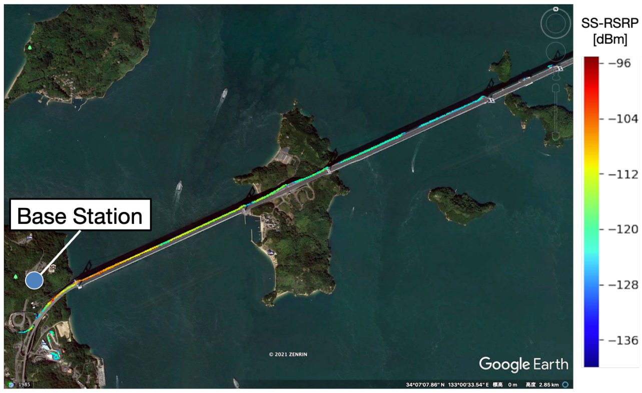

Fig. 8. Radio map of highest average SS-RSRP for each location.

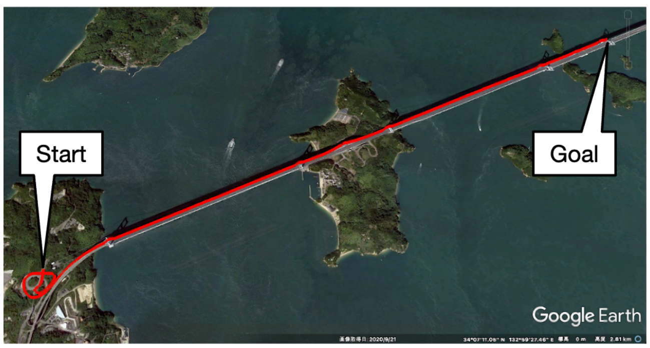

Fig. 9. GPS logs for analysis of fluctuation due to movement.

C. Comparison with Anchor Band Signal

Then, we compare the received signal power of the mmWave signal and the anchor band signal. In this paper, we have mapped the received signal power of mmWave and analyzed the highest average SS-RSRP in each beam. However, the construction of a spectrum database for mmWave signals has only just begun to be considered in this paper, and although it is expected that the number of related works will increase in the future, it will take some time to construct the database. On the other hand, database construction of microwave does not require each beam to be measured compared to mmWave, and most of the terminals are compatible with microwave band, so it is easy to measure by terminals. In the case where mmWave and microwave base stations are located in a short distance, we considered whether it is possible to predict the behavior of mmWave signals based on the measured values of microwave signals, which are easier to measure than mmWave signals. In this section, we compare the average received signal power (SS-RSRP, RSRP) of mmWave signals and microwave signals, assuming that the terminals move through the mesh along the same path, to verify the possibility of predicting the connectivity of mmWave signals from microwave signals. The movement path is from the start position to the goal position in Fig. 9 as in Sect. IV-B. Fig. 11 shows the fluctuation graph of the average received signal power (SS-RSRP, RSRP) of mmWave signals and microwave signals. From Fig. 11, it can

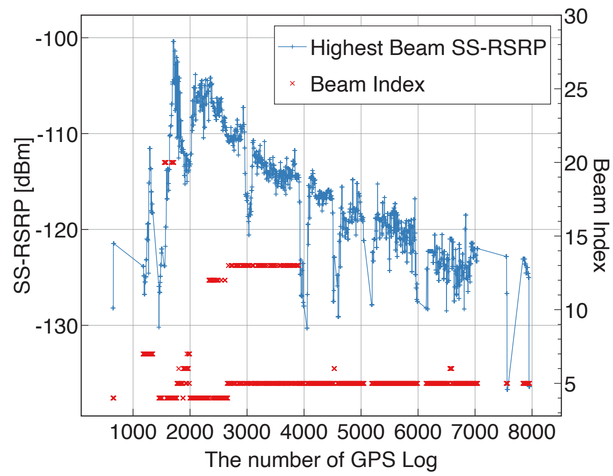

Fig. 10. Highest average SS-RSRP and index fluctuation in each beam index at each GPS log location.

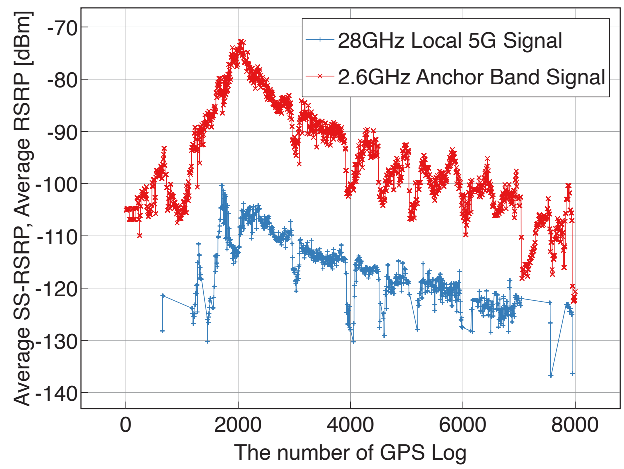

Fig. 11. Comparison of fluctuations in the average SS-RSRP of mmWave signals and the average RSRP of anchor band signals at each GPS log location.

be seen that the large-scale fluctuations of the average received power and the localized and sharp shadowing fluctuations after the GPS log number of 2000 are similar. Furthermore, at the points where the GPS log number is around 3000 and after 4000, there are few plots in the mmWave graph due to the mesh where there are no mmWave signal measurements due to the sharp drop caused by shadowing. On the other hand, in the microwave graph, the number of plots does not decrease even in the range where sharp attenuation occurs, and a dense plot can be confirmed. Thus, even when the mmWave signal power is less than the noise power and cannot be measured by the measurement equipment, it is possible to estimate the propagation and predict the connectivity of the mmWave signal by using the fluctuation of the microwave signal.

D. Comparison with Propagation Model

Finally, we evaluate the estimation error of the spectrum database. The errors between the estimated values from the database and the propagation model and the true values are

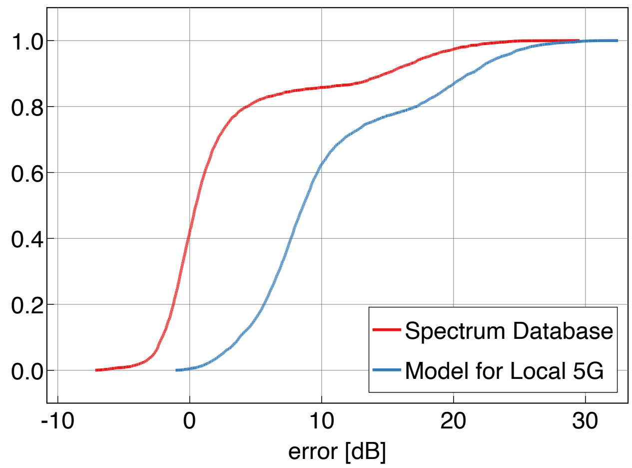

Fig. 12. Comparison of the CDF of the error between the database we constructed and the propagation model used for the local 5G license application.

compared, respectively. Here, the true values are defined as the instantaneous SS-RSRP values of a beam with beam index 4, measured on a single one-way measurement in the dataset. In this paper, the error is defined as the residual of the estimated value minus the true value. As a comparison, we consider the propagation model used to calculate the coverage area in the local 5G license application [14]. When utilizing mmWave frequencies, the propagation loss is basically based on Recommendation ITU-R P.1411. On the other hand, the free space path loss (FSPL) is used for line-of-sight propagation. Since the measurement environment in this paper is almost a line-of-sight propagation, FSPL was adopted for comparison. The received signal power P_{r} is expressed as follows:

$$P_{\mathrm{r}} = P_{\mathrm{t}} + G_{\mathrm{t}} - L_{\mathrm{f}} + G_{\mathrm{r}} - L_{\mathrm{FSPL}} - 4, \quad (1)$$

where P_{t} is the transmit power, but since the measurement parameter of the measurement campaign is SS-RSRP, it is necessary to obtain the transmit power per resource element. From the specifications of the local 5G base station (Nokia's AWEUA), the transmit power is 21 dBm at 100 MHz bandwidth, so the transmit power at 240 kHz bandwidth is about -5.2 dBm. Note that 240 kHz is the subcarrier spacing, which is the same as the bandwidth of one resource element. G_{t} is the transmit antenna gain, which is 23 dBi. L_{f} is the feed line loss of the base station, which is 3 dB. G_{r} is the receive antenna gain, which is -2.6 dB after subtracting the insertion loss of 5.6 dB for a 2 m cable from the antenna gain of 3 dBi. L_{FSPL} is the FSPL between the transmit and receive antennas.

The cumulative distribution function (CDF) of the error in the estimate is shown in Fig. 12. Fig. 12 shows that about 80% of the errors between the database estimate and the true value are within about ± 3 dB. On the other hand, the propagation model results in the CDF that is roughly 5 dB higher than the CDF of the database error. This can be interpreted to mean that the local 5G coverage area by the propagation model is designed to be extra, which confirms the usefulness of the propagation environment estimation by the database.

V. Conclusion

In this paper, we constructed a spectrum database of 28 GHz mmWave signals of local 5G base stations and analyzed the measurement results. By storing the measurement results in the spectrum database and statistically processing them, we were able to generate a radio map for each beam in the beamforming technique of 5G NR. We also clarified the beam index with the highest average SS-RSRP among the beams received at each mesh, the radio map of the highest average SS-RSRP, and the fluctuation with terminal movement, the relationship between the average received power of mmWave signals and anchor band signals, and comparison with propagation model. These results are expected to improve the performance of beam selection and handover selection methods.

Acknowledgment

This work was supported by the European Commission in the framework of the H2020-EUJ-02-2018 project 5GEnhance (Grant agreement no. 815056), by "Strategic Information and Communications R&D Promotion Programme (SCOPE)" of Ministry of Internal Affairs and Communications (MIC) of Japan (Grant no. JPJ000595). The authors would like to thank Ehime CATV, Inc. for their cooperation in the measurement campaign of the local 5G.

References

[1] Ericsson, "Ericsson mobility report," June 2021, [Online available] :https://www.ericsson.com/49e50d/assets/local/mobility-report/documents/2021/june-2021-ericsson-mobility-report.pdf [accessed 9 July 2021].

[2] F. C. Commission, "Spectrum policy task force report," *ETDocket No.02-135*, Nov. 2002.

[3] D. Makris, G. Gardikis, and A. Kourtis, "Quantifying tv white space capacity: A geolocation-based approach," *IEEE Communications Magazine*, pp. 145–152, Sept. 2012.

[4] K. Harrison, S. M. Mishra, and A. Sahai, "How much white-space capacity is there?" *2010 IEEE Symposium on New Frontiers in Dynamic Spectrum (DySPAN)*, May 2010.

[5] J. Mitola and G. Q. Maguire, "Cognitive radio: making software radios more personal," *IEEE Personal Communications*, vol. 6, no. 4, pp. 13–18, Aug. 1999.

[6] Q. Zhao and B. M. Sadler, "A survey of dynamic spectrum access," *IEEE Signal Processing Magazine*, vol. 24, no. 3, pp. 79–89, May 2007.

[7] I. F. Akyildiz, W. Lee, M. C. Vuran, and S. Mohanty, "A survey on spectrum management in cognitive radio networks," *IEEE Communications Magazine*, vol. 46, no. 4, pp. 40–48, Apr. 2008.

[8] T. Fujii and K. Umebayashi, "Smart spectrum for future wireless world," *IEICE Transactions on Communications*, vol. E100.B, no. 9, pp. 1661–1673, Sept. 2017.

[9] K. Sato, M. Kitamura, K. Inage, and T. Fujii, "Measurement-based spectrum database for flexible spectrum management," *IEICE Transactions on Communications*, vol. E98.B, no. 10, pp. 2004–2013, Oct. 2015.

[10] T. Fujii, "Smart spectrum management for v2x," *2018 IEEE International Symposium on Dynamic Spectrum Access Networks (DySPAN)*, pp. 1–8, Oct. 2018.

[11] A. Achtzehn, J. Riihijärvi, and P. Mähönen, "Improving accuracy for tvws geolocation databases: Results from measurement-driven estimation approaches," *2014 IEEE International Symposium on Dynamic Spectrum Access Networks (DYSPAN)*, pp. 392–403, Apr. 2014.

[12] C. Phillips, D. Sicker, and D. Grunwald, "Bounding the error of path loss models," *2011 IEEE International Symposium on Dynamic Spectrum Access Networks (DySPAN)*, pp. 71–82, May 2011.

[13] H. R. Imam, K. Inage, M. Ohta, and T. Fujii, "Measurement based radio environment database using spectrum sensing in cognitive radio," *2011 International Conference on Selected Topics in Mobile and Wireless Networking (iCOST)*, pp. 110–115, Oct. 2011.

[14] 5GMF, "Local 5g license application support manual (in japanese)," May 2021, [Online available] :https://5gmf.jp/wp/wp-content/uploads/2021/04/local-5g-manual2_02.pdf [accessed 1 Aug. 2021].